

OBSERVATIONS OF SUBSTORM ACTIVITY NEAR THE HARANG DISCONTINUITY

Irina Despirak, Tamara Kozelova, Boris Kozelov, Andris Lubchich

Polar Geophysical Institute, Apatity, Russia
e-mail: despirak@gmail.com

Keywords: Substorm, Westward and eastward electrojets, Brekup, Aurora, Harang discontinuity

Abstract: In our work we analyzed one interesting event, when the development of substorm injection occurs near the Harang discontinuity. It was the event, which was registered on 24 December 2014 from ~ 19: 00 to ~20:00 UT. Note, that this event was registered during very complicated conditions of space weather: there were series of shock waves, one of them was at the front of magnetic cloud (MC), and then the high speed stream (HSS) was observed. As result, two geomagnetic storms developed on 21 and 23 December 2014. We analyzed the substorm observed at the recovery phase of the second magnetic storm. The space-time dynamics of substorm was considered by simultaneous observations of the THEMIS satellites, the ground-based observations of aurora (MAIN camera system) and magnetic disturbances (IMAGE network) on the Kola Peninsula. During considered interval from ~ 19: 00 to ~20:00 UT, the THD was located at $|X| \sim 6 R_E$ and the projection of THD orbit crossed the Kola Peninsula. According to the THD data, four dipolarization fronts (DF) are distinguished and according to the IMAGE magnetometers data, the development of substorm occurs near the Harang discontinuity. It was shown that the pre-onset auroral forms were moved accordingly the two-cell ionospheric convection, which usually develop during the growth phase of the substorm.

НАБЛЮДЕНИЯ СУББУРЕВОЙ АКТИВНОСТИ ОКОЛО РАЗРЫВА ХАРАНГА

Ирина Дэспирак, Тамара Козелова, Борис Козелов, Андрис Любчич

Полярный геофизический институт, Апатиты, Россия
e-mail: despirak@gmail.com

Абстракт: В нашей работе мы проанализировали одно интересное событие, когда развитие суббуревой инжекции происходит вблизи границы Харанга. Это событие наблюдалось с ~19:00 до ~20:00 UT 24 декабря 2014 г. Отметим, что оно происходило в очень сложных условиях космической погоды: наблюдалась серия ударных волн, одна из них была на фронте магнитного облака (MC), а затем начался высокоскоростной поток (HSS). В результате 21 и 23 декабря 2014 развивались две магнитные бури. Мы исследовали суббуревую активность, наблюдавшуюся на фазе восстановления второй магнитной бури. Пространственно-временная динамика суббури рассматривалась с помощью одновременных наблюдений со спутников THEMIS, наземных наблюдений полярных сияний (система камер MAIN) и магнитных возмущений (сеть магнитометров IMAGE) на Кольском полуострове. В течение рассматриваемого интервала от ~ 19:00 до ~20:00 UT спутник THD располагался на $|X| \sim 6 R_E$, а проекция его орбиты пересекала Кольский полуостров. По данным спутника выделяются четыре фронта диполяризации (DF), по данным магнитометров IMAGE развитие суббури происходит вблизи разрыва Харанга. Показано, что предбурейкаповые авроральные формы двигались соответственно двухячейной ионосферной конвекции, которая обычно развивается на предварительной фазе суббури.

Introduction

The study of substorms, their dynamics and fine structure is important for the space weather investigations. The Harang discontinuity (HD) is an important part of the current systems in the case of the development of magnetic substorms [1], [2], [3]. Note, that the nature of the equivalent current systems of a magnetic substorm is formed by three sources: the eastward and westward electrojets flowing along the auroral oval and currents in the polar cap [4]. By using a large set of ground data (magnetometers, all-sky cameras, radars) and satellite observations, it was possible to establish that the Harang discontinuity is the complex structure that varies in space and time, depending on the time of day and season, and changing under the influence of conditions in the E layer of the ionosphere [5]. Fig. 1 shows the most common schemes of equivalent current systems in the ionosphere for cases of

substorms, which show the position of the Harang discontinuity. Fig 1a shows the scheme of currents, where the Harang discontinuity represents the transition between polar electrojets (the figure was taken from [6]). The scheme shows two types of substorms, corresponding to two types of the electrojets with currents of the opposite direction. Fig.1a corresponds to expansion substorms, when the electrojets are observed that converge closely in the evening-near midnight hours. Fig.1b corresponds to the case of convective substorms associated with the convection motions.

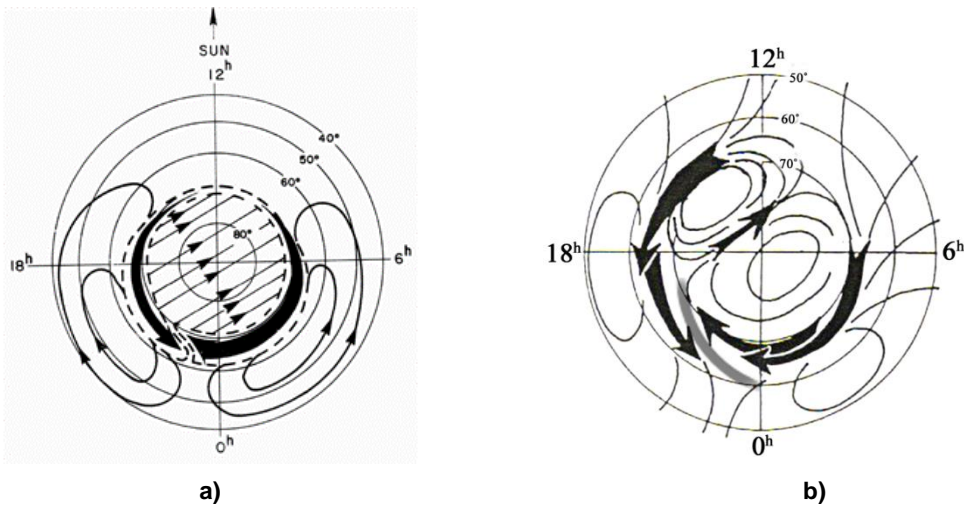


Fig. 1. The position of the Harang discontinuity on two diagrams of equivalent current systems a): transition between polar electrojets; b): reversal or reverse in the convection parameters. The picture was taken from [6].

However, it should be noted that despite a large number of studies, there is significant uncertainty regarding the space-time relations between the magnetosphere and the ionosphere during substorm expansions, and further research is needed using combined satellite and terrestrial data.

We found one interesting event, when the development of substorm injection occurs near the Harang discontinuity. It is the event on 24 December 2014, when simultaneous observations of the THEMIS satellites (THE and THD), the ground-based observations of aurora in Apatity and magnetic disturbances on the IMAGE magnetometers network and Russian Siberian stations (Dixon, Tiksi and Amderma) were available. Note, that the initial case of substorm activity in this day, during interval from ~ 16: 00 to ~ 17: 00 UT, was considered in our previous work [7]. During time interval from 14:30 to 20:50 UT on 24 December 2014, THE and THD satellites were located at $r \sim 8.0\text{--}10.3 R_E$ in the midnight sector of the magnetosphere and crossed over Siberia and Kola Peninsula. Fig.2 shown the geographic map with projections of the THD (red line) and THE (blue line) and the locations of magnetic stations. The first case of substorm activity (~ 16 ~ 17 UT) marked by a blue oval and inscription "1)"; the second case (19- 20 UT), marked as "2)".

In this work, we considered substorm activity from ~ 19: 00 to 20:00 UT, when THD was at a distance $|X| \sim 6 R_E$ in the plasma sheet, and its projection crossed the Kola Peninsula.

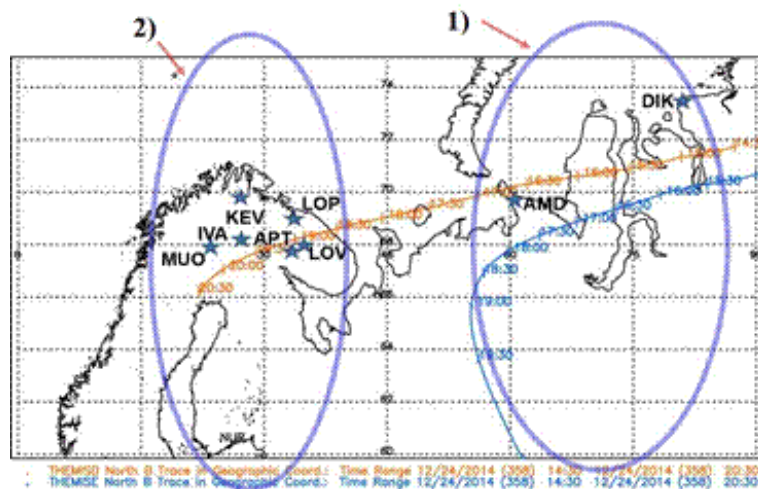


Fig. 2. Projections of the THD (red line) and THE (blue line) from 14:30 to 20:50 UT on 24 December 2014. The locations of magnetic stations are marked by stars, the time intervals under study - by blue ovals.

Data

For our analysis we used complex ground-based and satellites data. The solar wind and IMF parameters are taken from the CDAWeb database and the catalog of large-scale solar wind types <ftp://ftp.iki.rssi.ru/pub/omni/catalog> [8]. Global magnetometer networks IMAGE and SuperMAG, including data of Russian Siberian stations (Dixon, Tiksi, Amderma etc.) data were used for determination of the substorm development. The IMAGE magnetometer data are taken from <http://space.fmi.fi/image/>, SuperMAG magnetometers data - from <http://supermag.jhuapl.edu/> [9], [10]. Geomagnetic pulsations were observed by data from the induction magnetometer located in Lovozero. The data used here are the spectrograms in frequency range from 0.01 to 16 Hz, where the whole spectrum of natural pulsations Pi1B is well seen, if their existed. The auroras observations on MAIN cameras in Apatity (APT), to study the substorm development, we used the keograms and the selected full-frame images from the Apatity all-sky camera (APT, 67°34N; 33°24E). The camera specifications, their mutual location and the measurement process are described in detail in [11]. The variations of fields and particles in the magnetosphere were studied by THEMIS satellites (THD) data. During the time period from 19:00-20:00 UT the THD was located at $r \sim 6.3\text{--}8.5 R_E$, in the midnight sector: in 19:30 UT GSM coordinates were $(-6.3; 4.0; -1.06) R_E$.

1. Observations from THD satellite and Lovozero data

The data of FGM, EFI, SST, MOM instruments of the THD satellite are shown in the Figure 3a. It is seen that four dipolarization fronts (DF) were registered by THD data ($DF_1 = 19:18$; $DF_2 = 19:37$; $DF_3 = 19:45$, $DF_4 = 19:54$ UT). DFs were determined by sudden jumps of the magnitude and B_z component of the magnetic field, the strong variations in the electric field, the growth of the plasma velocity and the increasing of ion and electron fluxes (e.g. [12]). Four vertical black lines marked the DFs moments. As will be shown below, DF_1 was observed during the growth phase of the substorm, the last three dipolarization fronts were associated with the development of the expansion phase of the substorm and connected with brightening of arcs near the THD projection. In the Fig. 3b shown the Pi1B pulsations (the period $\tau = 0.2\text{--}15$ sec) observed in Lovozero. Note, that these pulsations are associated with substorm expansion phase and correlated with precipitations of auroral electrons. Three peaks of Pi1B pulsations were recorded in Lovozero: 19:22–19:25, 19:34–19:37 and 19:46–19:49 UT. The first peak was observed in connection with the appearance of beads at the growth phase arc located south of LOZ latitude. The second and third peaks were associated with the expansion phase of the substorm.

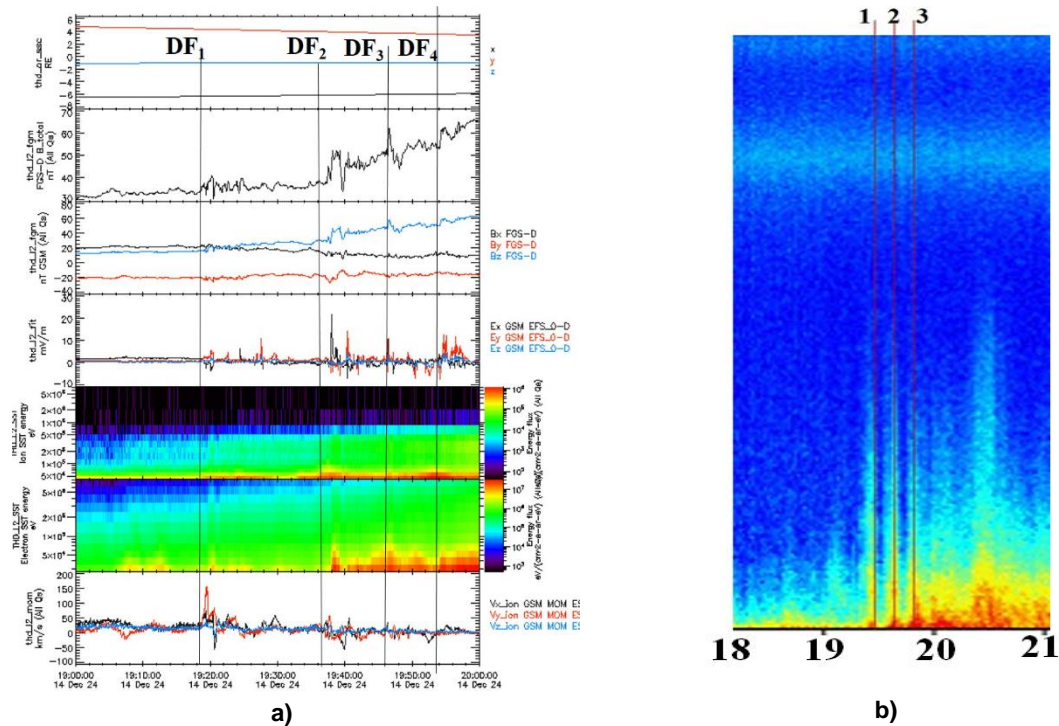


Fig. 3. Data of FGM, EFI, SST, MOM instruments of THD from 19:00 to 20:00 UT (a) and geomagnetic pulsations at Lovozero from 18 to 21 UT on 24 December 2014 (b). Moments of four dipolarization fronts (DF) marked by vertical black lines (a), moments of three peaks in Pi1B pulsations – by red vertical lines (b).

2. MAIN camera system observations

Auroral activity captured by all-sky camera at the station Apatity (APT) is presented in Fig. 4. Left three panels of Fig. 4 illustrate the temporal dynamics of the camera field of view as keogram: top panels - the keograms filtered by the horizontal-time difference and by the vertical-spatial difference; bottom panel - non-filtered keogram for interval 19:30 - 20:00 UT. Some selected images of all-sky camera are shown in Fig. 4b. During growth phase of substorm were registered "beads" in aurora ~ from 19:18 UT, which are visible both on the arc near the zenith and on the southern arc (picture not presented here). At this time, THD registered the first dipolarization front (DF_1) (Fig. 3a) and there were some weak disturbances in the ground-based magnetograms (Fig. 5a). Note, that the first peak in Pi1B pulsations at Lovozero was recorded a little later (~ 19:22 UT), when the auroras approached to LOZ latitude. At the end of the growth phase (~ 19:31:50 UT) a brightening of the most equatorial from all arcs was observed. Then on the arc, azimuthally spaced auroral folds are formed, moving from East to the West. This corresponds to the first phase of the breakup (or pseudo-breakup). At ~ 19:33:50 UT, the equatorial arc again became brighter, ~ 19:34 UT rapidly expand to the pole. This moment concerns to the onset of the second peak in Pi1B pulsations in LOZ (Fig. 3b). At ~ 19:37 UT (the maximum of second peak of Pi1B pulsations) an N-S arc occurred, then this arc moves equatorward and reaches E-W aligned arcs.

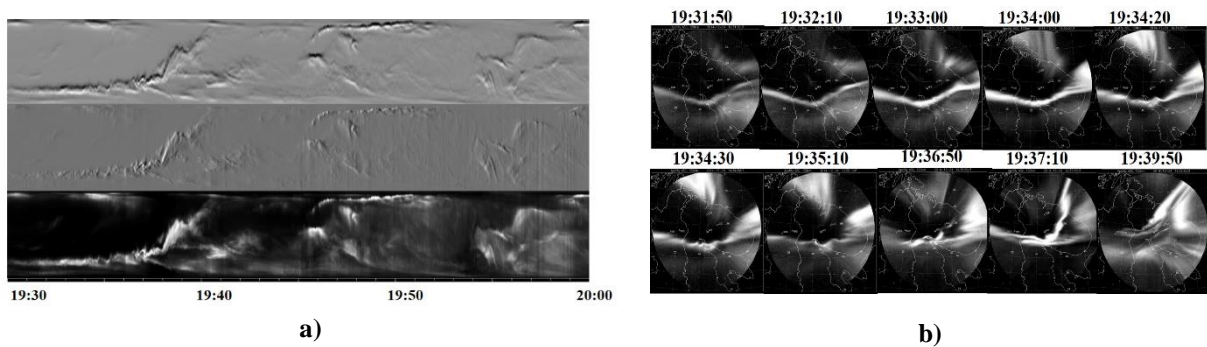


Fig. 4. Data of all-sky camera at the Apatity: a) keograms for time period from 19:30 to 20:00 UT: filtered (top panels) and non-filtered (bottom panel) keograms for 19:30-20:00 UT (a) and some images of all-sky camera for period 19:31:50-19:39:50 UT (b).

3. Ground-based magnetic observations

Fig. 5 presented the variations of X-component of magnetic field by IMAGE data. Vertical red lines corresponded to 3 moments of dipolarization fronts (DFs) registered by THD satellite (Fig. 3a), solid line DF_2 marked also the onset of expansion phase.

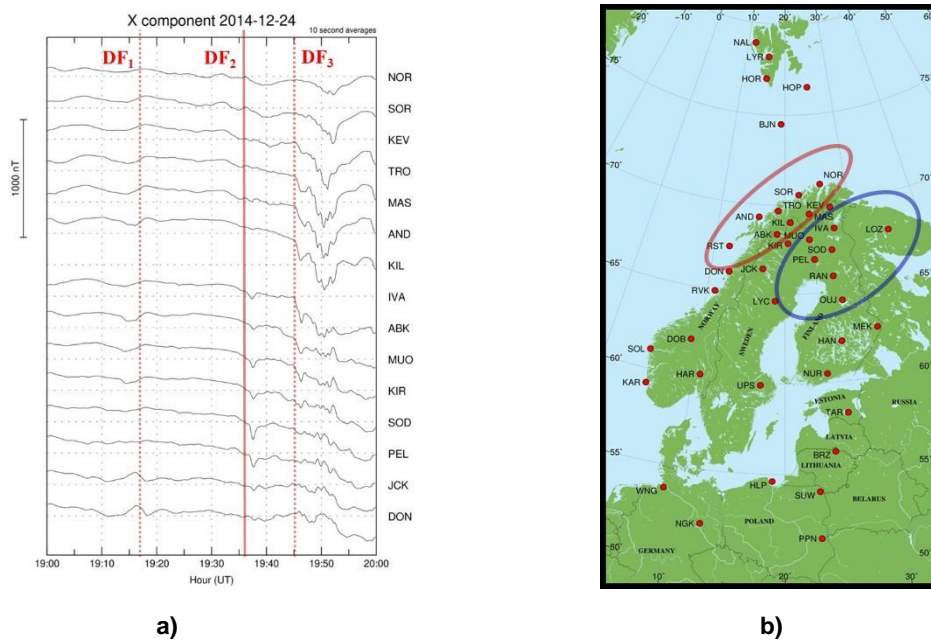


Fig. 5. X- component of geomagnetic field from IMAGE magnetometers, the DFs moments are marked by red vertical line (a); the map of locations of IMAGE magnetometers, red and blue ovals marked the region of positive and negative bays accordingly (b)

It is seen that near DF₂ moment were observed two different regions containing positive magnetic bays and negative magnetic bays, which marked also as red and blue ovals in the Fig. 5b. So, accordingly IMAGE magnetometers observations, the development of substorm occurs near the Harang flow shear.

Conclusions

Analysis of substorm activity using THD satellite data on / X / ~ 6 R_E and ground-based data led to the following results:

- 1) the fronts of dipolarization and injection of energetic electrons into the magnetosphere were observed near the moments of sudden intensification of auroras: brightening of arcs, breakup in aurora.
- 2) according to the magnetometers data, the development of substorm occurs near the Harang discontinuity
- 3) the development of aurora was organized according to the preceding two-vortex pattern of ionospheric convection observed in the growth phase around the Harang discontinuity.

Acknowledgements

The authors are grateful to the creators of the databases SuperMAG (SuperMAG: Products (jhuapl.edu)), IMAGE (<http://space.fmi.fi/image/>) for the opportunity to use them in this work. We are grateful to staff of Lovozero observatory of Polar Geophysical Institute for data of ground-based observations. THEMIS satellites data were taken from NASA CDAWeb <https://cdaweb.sci.gsfc.nasa.gov/cgi-bin/eval1.cgi>. We are grateful the heads of the experiments conducted with these instruments. The work was carried out within the framework of the State assignment for Polar Geophysical Institute (PGI).

References:

1. Harang, L., The mean field of disturbance of polar geomagnetic storms, *J. Geophys. Res.* 51(3), 353. doi:10.1029/te051i003p00353, 1946.
2. Kamide, Y., B.-H. Ahn, S.-I. Akasofu et al., Global distribution of ionospheric and field-aligned currents during substorms as determined from six IMS meridian chains of magnetometers: Initial results, *J. Geophys. Res.*, 87, doi: 10.1029/JA087iA10p08228, 1982.
3. Untiedt, J., W. Baumjohann, Studies of polar current systems using the IMS Scandinavian magnetometer array, *Space Sci. Rev.*, 63, 245–390, 1993.
4. Feldstein, Y. I., A. N. Zaitzev, Sd-variation of the magnetic field in high latitudes with different intensity of magnetic disturbances, *Annales Geoph.* 24, 2, 1–8. 1968.
5. Kunkel, T., J. Untiedt, W. Baumjohann, R. Greenwald, Electric fields and currents at the Harang discontinuity: a case study, *J. Geophysics*, 59. 73–86. 1986.
6. Zaitsev, A. H., K. Kh. Kanonidi, V. G. Petrov, Superposition of auroral currents in the region of the Harang discontinuity, *Geomag. Aeron.*, 62, 5, 607–616, 2022.
7. Despirak, I. V., Kozelova T. V., Kozelov B. V., Lubchich A. A. (2020) Westward propagation of substorm by THEMIS and ground-based observations, *J. Atmosph. Solar-Terr. Phys.*, 206, № 105325. doi: 10.1016/j.jastp.2020.105325.
8. Yermolaev, Yu. I., N. S. Nikolaeva, I. G. Lodkina, M. Yu. Yermolaev, Catalog of large-scale solar wind phenomena during 1976–2000, *Cosmic Res.*, 47, 2, 81–94, 2009.
9. Viljanen, A., L. Häkkinen, IMAGE magnetometer network, Satellite-ground based coordination sourcebook, ed. Lockwood M., Wild M. N., Opgenoorth H.J. ESA publications SP-1198, 111–117. 1997.
10. Gjerloev, J. W. The SuperMAG data processing technique, *J. Geophys. Res.*, 117(A9), A09213, 2012, <https://doi.org/10.1029/2012JA017683>
11. Kozelov, B. V., Pilgaev S. V., Borovkov L. P., Yurov V. E., Multi-scale auroral observations in Apatity: winter 2010-2011, *Geosci. Instrum. Method. Data Syst.*, 1, 1–6, doi:10.5194/gi-1-1-2012, 2012.
12. Kozelova, T. V., B. V. Kozelov, Substorm-associated explosive magnetic field stretching near the earthward edge of the plasma sheet, *J. Geophys. Res.: Space Physics*, 118(6), 3323–3335, doi:10.1002/jgra.50344, 2013.